## Uncoupling of calcium channel alpha(1) and beta subunits in developing neurons

Spafford, J.D.; van Minnen, J.; Larsen, P.; Smit, A.B.; Syed, N.I.; Zamponi, G.W.

***published in***
Journal of Biological Chemistry
2004

***DOI (link to publisher)***
10.1074/jbc.M403781200

***document version***
Publisher's PDF, also known as Version of record

THE JOURNAL OF BIOLOGICAL CHEMISTRY
Vol. 279, No. 39, Issue of September 24, pp. 41157–41167, 2004

*Printed in U.S.A.*

# Uncoupling of Calcium Channel $\alpha_1$ and $\beta$ Subunits in Developing Neurons*

Received for publication, April 5, 2004, and in revised form, July 16, 2004
Published, JBC Papers in Press, July 20, 2004, DOI 10.1074/jbc.M403781200

**J. David Spafford‡, Jan van Minnen§, Peter Larsen¶, August B. Smit§, Naweed I. Syed‡‖**, and Gerald W. Zamponi‡‖‡‡**

*From the ‡Cellular and Molecular Neurobiology Research Group, University of Calgary, Calgary T2N 4N1, Canada, the §Department of Molecular and Cellular Neurobiology, Research Institute Neurosciences, Vrije Universiteit, 1081 HV Amsterdam, The Netherlands, and the ¶Department of Clinical Neurosciences, University of Calgary, Calgary T2N 4N1, Canada*

**Calcium channel $\beta$ subunits are key modulators of calcium channel function and membrane targeting of the pore-forming $\alpha_1$ subunit. Here we show that an invertebrate (*Lymnaea stagnalis*) homolog of P/Q- and N-type calcium channels ($LCa_v2$), although colocalized with $\beta$ subunits in synapses of mature neurons, is physically uncoupled from the $\beta$ subunits in the leading edge of growth cones of outgrowing neurons. Moreover, $LCa_v2$ channels that mediate transmitter release in mature synapses also participate in neuronal outgrowth in growth cones. The differential association of $\beta$ subunits with synaptic calcium channels and those expressed in emergent neuronal growth suggests that $\beta$ subunits may play a role in the transformation of $Ca_v2$ calcium channel function in immature neurons and mature synapses.**

Members of the $Ca_v2$ calcium channel family are considered essential triggers of synaptic transmission at vertebrate (1) and invertebrate synapses (2–4). Like other types of high voltage-activated channels, $Ca_v2$ channels exist as macromolecular complexes of a pore-forming $\alpha_1$ subunit and ancillary $\beta$, $\alpha_2$-$\delta$, and possibly $\gamma$ subunits (5). The mammalian brain expresses four different types of $\beta$ subunits that interact to differentially modulate $\alpha_1$ subunit function (6, 7). The functional effects of $\beta$ subunit coexpression include changes in the voltage dependences and rates of activation and inactivation, plus an increase in current densities (8–17). The latter observation has been linked to the masking of an endoplasmic reticulum (ER)[1] retention signal on the calcium channel $\alpha_1$ subunit (18). The physiological importance of calcium channel $\beta$ subunits is supported by studies involving mutant and knockout mice. For example, a spontaneous mutation in $\beta_4$ effectively leads to a functional null mouse resulting in a lethargic phenotype with impaired synaptic transmission (19). Alternatively, knockout of $\beta_3$ inhibits the activities of neuronal L-type and N-type channels (20). However, because the central nervous system expresses multiple $\beta$ subunits, compensation by other $\beta$ subunit isoforms complicates the analysis of these phenotypes (21). Moreover, synaptic nerve terminals frequently express both N-type and P/Q-type calcium channels (22), each of which can associate with all of the four $\beta$ subunits (23–25). This combinatorial subunit complexity has hampered attempts to delineate the precise fundamental roles of $\beta$ subunits on synaptic function (21).

In contrast, invertebrates express only a single representative of each of the three major calcium channel $\alpha_1$ subunit isoforms and a singleton homolog of the $\beta$ subunit (26). We have reported recently the isolation and functional characterization of a $Ca_v2$ calcium channel homolog ($LCa_v2$) from the mollusc *Lymnaea stagnalis*. We showed that $LCa_v2$ displays functional properties that are reminiscent of mammalian N-type calcium channels (27) and that this channel is essential for synaptic transmission between identified *Lymnaea* neurons (4). Like its vertebrate counterpart, $LCa_v2$ contains the $\alpha$-interaction domain, a highly conserved region in the domain I–II linker that is essential for interactions with calcium channel $\beta$ subunits (4, 27). Furthermore, the *Lymnaea* model system allows for the *in vitro* reconstruction of identified synapses, which are highly amenable for molecular and cellular manipulation. These synapses are target cell-specific, require gene transcription and *de novo* protein synthesis, are ultrastructurally and electrophysiologically similar to those observed *in vivo* (28, 29), and will establish appropriate synapses *in vivo* after transplantation into the intact ganglia (28, 30). In this study, we took advantage of this invertebrate model to elucidate fundamental aspects of $\beta$ subunit physiology.

Here we report the isolation of the *Lymnaea* $\beta$ subunit ($LCa_v\beta$), its functional characterization, and its distribution in neurons. $LCa_v\beta$ caused neither a considerable alteration in $LCa_v2$ calcium channel activity nor did it mediate an increase in expression of $LCa_v2$. We show that besides their known function in triggering neurotransmitter release, $LCa_v2$ channels are essential for proper synaptic outgrowth. However, in terminal growth cones and nascent growth along major neurites, $\beta$ subunits are spatially and physically uncoupled from $LCa_v2$ channels and not associated with neurite outgrowth. In synaptic contacts, $LCa_v2$ channels associate with $\beta$ subunits that potentially are synthesized locally in distal neurites. This local pool of neuritic $\beta$ subunits may support the immediate and cytoskeletal reorganization of the developing growth cone

* This work was supported in part by operating grants from the Canadian Institutes of Health Research (to G. W. Z. and N. I. S.). The costs of publication of this article were defrayed in part by the payment of page charges. This article must therefore be hereby marked "*advertisement*" in accordance with 18 U.S.C. Section 1734 solely to indicate this fact.

‖ Canadian Institutes of Health Research Investigator.
** Recipient of a Scientist award from the Alberta Heritage Foundation for Medical Research.
‡‡ Recipient of Senior Scholar award from the Alberta Heritage Foundation for Medical Research, a Canada Research Chair award, and an Independent Investigator award from the National Alliance for Research on Schizophrenia and Depression. To whom for correspondence should be addressed: Dept. of Physiology and Biophysics, University of Calgary, 3330 Hospital Dr. NW, Calgary T2N 4N1, Canada. Tel.: 403-220-8687; Fax: 403-210-8106; E-mail: Zamponi@ucalgary.ca.

[1] The abbreviations used are: ER, endoplasmic reticulum; PBS, phosphate-buffered saline; HA, hemagglutinin; SH, Src homology; r, rat; RNAi, RNA interference.

into a nascent synapse or the dynamic remodeling in mature synapses.

## EXPERIMENTAL PROCEDURES

*Molecular Identification, Structural Analyses, and Preparation of Lymnaea Genes for in Vitro Expression*—The *L. stagnalis* calcium channel β subunit $LCa_v\beta$ (gi:29378324) was identified in a 418-bp PCR product from fresh *Lymnaea* brain cDNA with the use of degenerate primers (4). The isolated PCR product served as a probe to isolate a full-length 1950-bp cDNA homolog coding for $LCa_v\beta$ (gi:29378324) from *Lymnaea* brain cDNA libraries (Vrije Universiteit Amsterdam, The Netherlands). Protein sequences of $LCa_v\beta$ and other $Ca_v\beta$ subunit homologs were aligned in PILEUP (GCG Wisconsin Package, Accelrys) and imported into PAUP 4.0 to generate a consensus gene tree using the Branch-and-Bound algorithm. The gene tree was tested for robustness in 100 bootstraps and displayed in TREEVIEW 1.6.6 (Rod Page, Glasgow, Scotland, UK). A running window of average similarity of the aligned genes was displayed using PLOTSIMILARITY (GCG Wisconsin Package).

For *in vitro* expression, 5′ NotI and 3′ XhoI restriction sites were incorporated into primers flanking the 568-amino acid coding region of $LCa_v\beta$ for PCR cassette insertion into the mammalian expression vector PMT2SX. The sequence immediately upstream from the start (ATG) codon was also altered to include a consensus Kozak sequence CGGCCGCCACC(ATG).

*Transfection and Assessment of Function in Vitro by Patch Clamp Electrophysiology*—Heterologously expressed cDNAs encoding an enhanced green fluorescent protein marker (Clontech), a $Ca_v2$ $\alpha_1$ subunit from rat ($rCa_v2.1$, $rCa_v2.2$, and $rCa_v2.3$) or *Lymnaea* ($LCa_v2a$, GenBank™ accession number AF484082), the rat $\alpha_2$-$\delta_1$ subunit, and either no β subunit or one of the four rat β subunits ($\beta_{1b}$, $\beta_{2a}$, $\beta_3$, and $\beta_4$) or the *Lymnaea* β subunit ($LCav\beta$) were transfected into human embryonic kidney *tsA-201* cells by using a standard calcium phosphate protocol (27). Transfected $LCa_v2a$ cDNA contained the first 44 amino acids swapped with the homologous region of rat $Ca_v2.1$. We demonstrated previously (27) that this alteration is one that is both necessary and sufficient for membrane expression of $LCa_v2a$ in human cell lines. The activities of calcium channels were measured with barium as the charge carrier via whole cell patch clamp using an Axopatch 200B amplifier (Axon Instruments, Union City, CA), pCLAMP 9.0 software, after incubation of transiently transfected cells at 28 °C for 2–4 days. All solutions and recording procedures have been described previously (27).

Electrophysiological data were analyzed in Clampfit (pClamp 9, Axon Instruments) and SigmaPlot 2000 (Jandel Scientific, SPSS Science, Chicago). Steady state inactivation curves and macroscopic current voltage relations were analyzed using a standard Boltzmann equation. A monoexponential fit of the raw data was used to derive time constants for inactivation and for recovery from inactivation. Data are expressed as means ± S.E., with numbers in parentheses, as displayed in the figures, reflecting the numbers of experiments. Statistical analysis was carried out using Sigmastat (Jandel Scientific). Differences between mean values from each experimental group were tested using paired and unpaired Student's *t* tests or one-way analysis of variance and were considered significant if $p < 0.05$.

*Polyclonal Antibody Synthesis and Immunolocalization of Lymnaea $LCa_v\beta$ and $LCa_v2$ in Cultured Neurons and Transfected Cell Lines*—The peptide SLDEEKEALRRET corresponding to amino acids 64–76 (see Fig. 1*A*) was used as the antigen for the $LCa_v\beta$ peptide antibody. Matrix-assisted laser desorption ionization-mass spectrometry and analytical high pressure liquid chromatography were used to confirm the purity of the peptide (Henk Hilkman, Netherlands Cancer Institute, Amsterdam, The Netherlands). Rabbits were immunized for a 4-week period with adjuvants and antigen conjugated to carrier protein (Washington Biotechnology Inc., Baltimore). Rabbit antiserum was enzyme-linked immunosorbent assay titered at 1:50,000 and measured for immunoreactivity by spot blot. A peptide polyclonal antibody for the $LCa_v2$ calcium channel was derived from the antigenic sequence KAEDNENDSEQNDND, coding for amino acids 418–432 of the cytoplasmic I–II linker. This peptide coupled to carrier was raised either as anti-rabbit (27) or anti-chicken.

Western blot samples consisted of proteinaceous extracts of harvested transiently transfected or untransfected *tsA-201* cells incubated for 4 days at 37 °C or freshly isolated *Lymnaea* central ring ganglia. Cell samples were collected on ice in 500 μl of 0.32 M sucrose and the protease inhibitors pepstatin A (1 mg/ml), aprotinin (1 mg/ml), leupeptin (1 mg/ml), pefabloc SC (0.2 mM), benzamidine (0.1 mg/ml), and the calpain inhibitors I and II (8 mg/ml each). After centrifugation, supernatants of proteinaceous extracts were separated by 5% SDS-PAGE and transferred (40 V for 16 h) onto a Immobilon polyvinylidene difluoride membrane (Millipore). After air-drying for 2 h, the membranes were blocked for nonspecific binding in 5% milk, 0.1% Tween 20, PBS solution (137 mM NaCl, 2.7 mM KCl, 4.3 mM $Na_2HPO_4$, 1.4 mM $KH_2PO_4$ (pH 7.3)) and incubated overnight at 4 °C in primary antibody (1:2000). The membranes were washed five times in PBS/Tween 20 followed by incubation for 1 h with goat anti-rabbit or donkey anti-chicken IgG-coupled horseradish peroxidase in 5% milk/PBS/Tween 20 and five washes in PBS/Tween 20. Antigen was detected using chemiluminescent horseradish peroxidase substrate (ECL, Amersham Biosciences) and visualized following exposure to Amersham Hyperfilm-MP.

Neurons (VD4, LPeD1, RPeD1, CGCs) that form identified synapses *in vitro* were isolated from the *Lymnaea* central ring ganglia by using established protocol (4, 28) and plated on poly-L-lysine-coated substrate for 48 h in brain-conditioned medium at a density to foster both growth cone development in singletons and synaptically connected neurite-neurite pairs in the same dish. Immunolabeled samples of untransfected/transfected *tsA-201* and identified *Lymnaea* cultured cells were fixed using 1% paraformaldehyde, permeabilized, and blocked in 0.1% Triton X-100, 1 g/liter bovine serum albumin containing 0.05 M Tris buffer, pH 7.4. Immunolabeled samples were washed extensively in Tris/bovine serum albumin/Triton followed by washing in Tris buffer (27). Immunolabeled samples were exposed to primary (1:2000 dilution) and fluorescently conjugated secondary antibodies overnight at 4 °C for 45 min at room temperature, respectively, to limit background staining. Background staining was assessed by preincubating the peptide polyclonal antibody at 1:2000 dilution with the antigenic peptide (5 μg/ml) overnight or by substituting the primary antibody for anti-rabbit or anti-chicken preimmune serum at 1:2000. Fluorescently conjugated secondary antibodies for immunostaining IgG (H+L) anti-rabbit $LCa_v\beta$, and anti-rabbit or anti-chicken IgG (H+L) $LCa_v2$ consisted of Alexa Fluor 555 (red) donkey anti-rabbit IgG or Alexa Fluor 488 (green) goat anti-chicken IgG at 1:400 dilution (Molecular Probes, Inc., Eugene, OR). Prepared samples were wet-dried and mounted in fluorescence antifading media (Fluorsave, Calbiochem). Images were visualized and analyzed on an Olympus confocal microscope.

*In Situ Hybridization and Immunolocalization in Lymnaea Central Ring Ganglia Sections—Lymnaea* central nervous systems were fixed in Bouin's fixative (16–24 h) and, after dehydration with ethanol, embedded in paraffin. Consecutive 7-μm sections were adhered to Superfrost™ microscope slides.

$LCa_v\beta$ RNA was detected in tissue sections with run-off antisense RNA, complementary to the coding region of amino acids 114–354 (720 bp) of $LCa_v\beta$. An antisense construct was synthesized in the PCR by using forward primer with a 5′ incorporated KpnI site, GGGGTACCTGGCTGTGCGGTGTCATTTGGGG, upstream of DNA position 505 bp and 3′ reverse primer, GATTGTGTCACAGTCCAACACCAC, ending at position 1260 bp just downstream of a unique SacI restriction site at 1229 bp. The resulting PCR product after KpnI-SacI digestion was inserted into pBluescriptII KS+. EV3 and EV2 primers were used to amplify the 721-bp PCR product containing the $LCa_v\beta$ fragment flanked by T7 and T3 promoters of pBluescript KS+. RNA was synthesized from this linear PCR template using T7 (for sense probe) and T3 (for antisense probe) RNA polymerase (Roche Applied Science). RNA probes were then labeled with $^{35}$S-dUTP (PerkinElmer Life Sciences) rendering specific activities of >50000 cpm/pmol DNA. The 10 fmol/μl probe in a standard hybridization mixture was incubated overnight at 37 °C and then washed with increasing stringencies at 60 °C. Slides were subsequently dipped in Eastman Kodak NTB2 emulsion and developed after 7 days of autoradiographic exposure.

*Assessment of RNA Transcript Levels and Local Protein Expression in Isolated Neurites*—Isolated *Lymnaea* CGC neurons were isolated and subsequently cultured on a poly-L-lysine-coated adhesive substrate as described previously (31). Briefly, neurons were plated with long neuritic stumps to maximize neurite extension without allowing neuronal intra-connections (autapses) or inter-connections with other neurons (synapses). After 2 days of culturing, somata were severed from neurites with a sterile glass pipette 20–40 μm from the somata and then removed from the dish.

For reverse Northern blot analyses, dishes containing soma-ablated neurites were rinsed three times in sterile saline before cultured neurites were bathed and lifted from the adhesive substrate by trituration in Trizol reagent (Invitrogen). Subsequent to Trizol extraction, total RNA (200 ng) was amplified by SMART cDNA synthesis (zco;clontech-Clontech). Blots were probed with $^{32}$P-labeled/PCR-amplified cDNA inserts spotted with DNA plasmids (200 ng) on a Hybond-N nylon membrane (Amersham Biosciences) coding for DNA fragments of *Lym-*

*naea* calcium and potassium channel clones (GenBank™ accession number, corresponding to the amino acid sequences, *$LCa_v1$* (AF484079, 373–670), *$LCa_v2$* (AF484082, 302–621), *$LCa_v3$* (AF484084, 848–1111), *$LCa_v\beta$* (AF484087, 285–433), *$LK_v2.1$* (AY551910), and *$LK_v3.1$* (AY551911), and subsequently imaged via a PhosphorImager (Bio-Rad). *$LK_v2.1$* and *$LK_v3.1$* are novel sequences accompanying this paper that were isolated from fresh *Lymnaea* cDNA by degenerate PCR.

To assess local protein synthesis of *$LCa_v\beta$* mRNA in soma-ablated neurites, an HA-tagged *$LCa_v\beta$* construct was designed by nested PCR insertion of TACCCATACGATGTTCCAGATTAC, coding for an HA epitope (YPYDVPDY) just downstream of the start codon of full-length *$LCa_v\beta$* in pBluescript II KS+. Linearized template was created by digestion of post-3′-untranslated region of linearized HA-tagged *$LCa_v\beta$* with KpnI enzyme. *In vitro* transcribed, capped, and poly(A)-tailed RNA was synthesized from 3′ linearized HA-tagged *$LCa_v\beta$* construct plasmid using the mMessage mMachine T7 Ultra kit (Ambion, Austin, TX). HA-tagged *$LCa_v\beta$* mRNA construct was microinjected into soma-ablated neurites, followed by a 12-h incubation to allow heterologous expression of HA-tagged protein. These samples were then fixed and stained for HA epitope using a rat monoclonal antibody (clone 3F10, Roche Applied Science), followed by Alexa Fluor 488-conjugated chicken anti-rat IgG (H+L), using the immunocytochemical procedure described above.

*Gene Knockdowns in Cultured, Identified Lymnaea Neurons*—Gene knockdowns were carried out on isolated CGC neurons, plated on non-adhesive, hemolymph-treated glass coverslips, and bathed in brain-conditioned medium with 10 μM antisense/mismatch DNA oligonucleotide probes (4, 32) or 10 μg of double-stranded RNA (4). After 3 days of incubation, the treated neurons were transferred to poly-L-lysine-pretreated glass coverslips bathed in fresh brain conditioned medium. These neurons were incubated for 48 h in the dark to maximize sprouting of neurites and then fixed in 1% paraformaldehyde and immunostained for detection of *$LCa_v2$* and *$LCa_v\beta$* protein expression by confocal microscopy. Extension of primary neurites beyond five somata lengths was considered normal, control neurite growth.

15-mer antisense ACAAGACGACCTATC spanned a region of a highly conserved sequence at amino acids 136–141, coding for WIGRLV at position 574–588 bp in *$LCa_v\beta$*. Mismatch probes for *$LCa_v\beta$* consisted of 3 base changes to the antisense sequence, ACGAGACCACCGATC (changed nucleotides are underlined). Antisense/mismatch probes were prefiltered through a 0.8-μm filter, boiled for 2 min, and cooled on ice before incubation with neurons. Fluorescence intensities of antisense *versus* mismatch *$LCa_v\beta$* samples were quantified in optical density units in a 200 × 200 μm area encompassing each neuron centered in view using ImageJ software (National Institutes of Health).

As described previously (4), RNA interference probes consisted of a mixture of double-stranded RNA synthesized by T7/T3 transcription in both sense/antisense strands (MEGASCRIPT; Ambion, Austin, TX) of template inserted between T7 and T3 promoters in Bluescript II KS+ vector. The template coded for the II–IIII loop in *$LCa_v2a$* (2237–2710) and *$LCa_v2b$* (2237–2761), or a negative control consisting of a fragment of the 3′-untranslated region of *$LCa_v2$* that lies between natural PstI and HindIII sites (6709–7278). All of the experiments involving gene knockdown were carried out in a double blind fashion.

## RESULTS

*Lymnaea Neurons Express a $Ca_v\beta$ Subunit*—A full-length 1950-bp cDNA homolog coding for a 568-amino acid calcium channel β subunit (*$LCa_v\beta$*) was isolated from an *L. stagnalis* brain cDNA library (Fig. 1*A*). Other invertebrates as well as completed genomic sequences of *Caenorhabditis elegans* and *Drosophila* reveal a similar singleton homolog that represents the four known mammalian β subunit isoforms (*i.e.* $\beta_1$ through $\beta_4$, Fig. 1*B*). *$LCa_v\beta$* and mammalian β subunits display a similar architecture of three variable regions separated by two highly conserved regions, in which *$LCa_v\beta$* and mammalian β subunits share 80 and 89% sequence identity, respectively (Fig. 1, *A* and *C*). The β subunit core is considered to resemble central modules of membrane-associated guanylate kinase homologs (33–35), with conserved and interacting SH3 and guanylate kinase domains, and a variable HOOK region that splits the SH3 fold (Fig. 1, *A* and *C*). Residues in the guanylate kinase domain contribute to form a deep, hydrophobic groove for high affinity binding of high voltage-activated calcium channels (33, 35), which are highly conserved residues among invertebrate and mammalian β subunits (Fig. 1*A, black residues*).

The striking conservation of the structural core of all invertebrate and vertebrate β subunits suggests a functional equivalency of the four mammalian β subunits with the singleton invertebrate homolog. At vertebrate presynaptic terminals, all four mammalian β subunit isoforms are considered potential regulators of the two synaptic calcium channel $\alpha_1$ subunits, P/Q-type ($Ca_v2.1$) and N-type ($Ca_v2.2$). Like the singleton β subunit gene, invertebrates bear a single $Ca_v2$ homolog that represents both mammalian P/Q-type and N-type synaptic calcium channels and that is essential for synaptic transmission (26). This lack of combinatorial complexity of multiple calcium channels and β subunits provides for a unique opportunity to delineate the fundamental neurophysiological function of the β subunit.

*Distribution of $LCa_v\beta$ in Lymnaea Brain*—To assess the distribution of *$LCa_v\beta$* and its putative colocalization with the *$LCa_v2$* calcium channel $\alpha_1$ subunit in *Lymnaea* brain, we generated a polyclonal peptide antibody designed against the β subunit raised in rabbit (see Fig. 1, *A* and *C*), and an anti-chicken *$LCa_v2$* antibody, whose epitope specificity was characterized previously from rabbit (27). As shown in Fig. 2, the anti-rabbit β subunit (Fig. 2*A*) and anti-chicken *$LCa_v2$* calcium channel $\alpha_1$ subunit (Fig. 2*B*) antibodies recognized appropriate sized bands in Western blots containing extracts from either transfected *tsA-201* (*$LCa_v\beta$*) or *Lymnaea* central nervous system (*$LCa_v\beta$* and *$LCa_v2$* $\alpha_1$). Whereas the β subunit antibody recognized a single, expected ~62-kDa protein, two bands representing the previously described *$LCa_v2$* isoforms (4), a full-length (~243 kDa) variant, *$LCa_v2a$,* and a short, C-terminally truncated (~185 kDa) variant, *$LCa_v2b$,* were identified with the anti-chicken *$LCa_v2$* $\alpha_1$ subunit antibody. Additionally, both antibodies produced robust membrane staining in *tsA-201* cells cotransfected with *$LCa_v\beta$* and the *$LCa_v2$* $\alpha_1$ subunit (Fig. 2*C*).

The two subunits showed overlapping distribution in the plasma membrane, consistent with the formation of a channel complex. Overnight preincubation of the antibody with 5 μg/ml peptide used as the epitope for antibody generation of *$LCa_v2$* or *$LCa_v\beta$* with their primary antibody removed virtually all of the staining in both tsA-201 cells and in cultured neurons (not shown). Specificity was further confirmed by the dense *$LCa_v2$* and *$LCa_v\beta$* antibody costaining in cultured neurons (Fig. 4, *C–E*) compared with preimmune controls (Fig. 4, *A* and *B*). Collectively, these data are consistent with findings in vertebrate neurons that presynaptic calcium channels are complexed with ancillary β subunits (24, 25).

*$LCa_v\beta$ Weakly Regulates $LCa_v2$ Properties*—Despite the apparent overlap in membrane expression shown in Fig. 2*C*, there was a striking lack of regulation of biophysical properties of *$LCa_v2$* by *$LCa_v\beta$*. In contrast to what has been reported for mammalian β subunits (8–17), *$LCa_v\beta$* did not affect the voltage dependences of activation (Fig. 3*A*) and inactivation (Fig. 3*C*), and there was no effect on the kinetics of recovery from inactivation (Fig. 3*D*). Moreover, there was no effect on current densities (Fig. 3*B*), suggesting that *$LCa_v\beta$* may not affect membrane expression of the *$LCa_v2$* $\alpha_1$ subunit. The only measurable effect of *$LCa_v\beta$* was a slight but statistically significant slowing of the inactivation kinetics (Fig. 3, *E* and *F*). We therefore conclude that *$LCa_v2$* activity is only weakly regulated by *$LCa_v\beta$*.

To rule out the possibility that *$LCa_v\beta$* was perhaps not functionally expressed in *tsA-201* cells, and to determine whether *$LCa_v2$* simply lacked a general ability to functionally interact with β subunits, we examined various combinations of rat and *Lymnaea* $\alpha_1$ and β subunits. As shown in Fig. 3, mammalian β

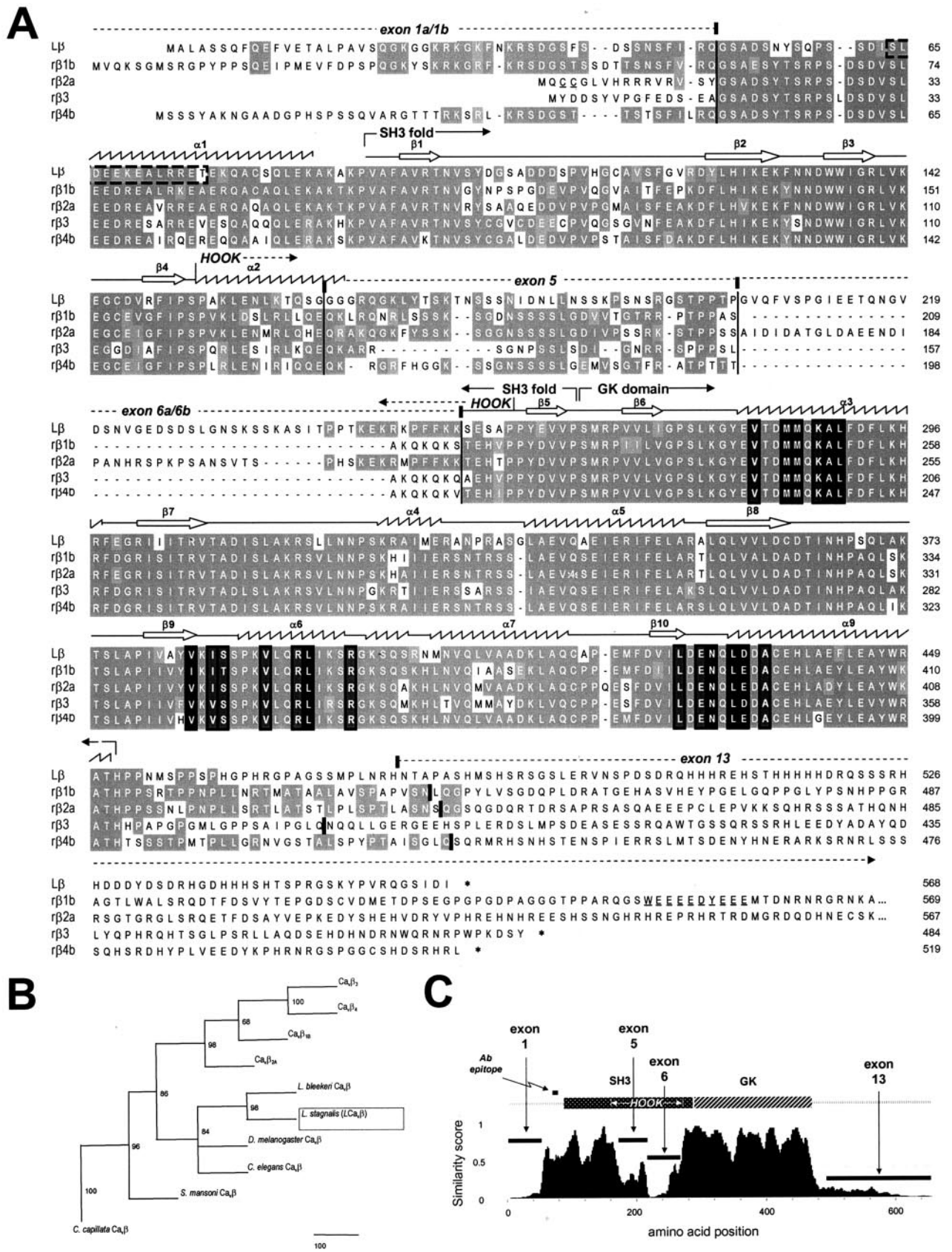


FIG. 1. **Structural comparisons between β subunit isoforms.** *A*, alignment between *Lymnaea* $Ca_v\beta$ and the four rat β subunit subtypes. Identical amino acids are indicated by *dark outlined gray boxes* and similar ones by *lighter colored gray boxes*. Putative locations of α helices and β sheets are provided from current structural models (33). Residues lining a hydrophobic groove of β subunits that are considered to interact directly with $\alpha_1$ subunits of $Ca_v1$ and $Ca_v2$ calcium channels are *darkly shaded* conserved residues (33, 35). *B*, most parsimonious gene tree of β subunits generated from the four rat orthologs and singleton invertebrate representatives. *Numbers* at branch node represent robustness of branches in 100 bootstraps. *C*, running window of similarity among invertebrate and rat homologs illustrated in *B*. Note the highly conserved core of β subunits in SH3 and guanylate kinase (*GK*) domains and the variable HOOK domain that splits the SH3 domain. Highly divergent exons 1,

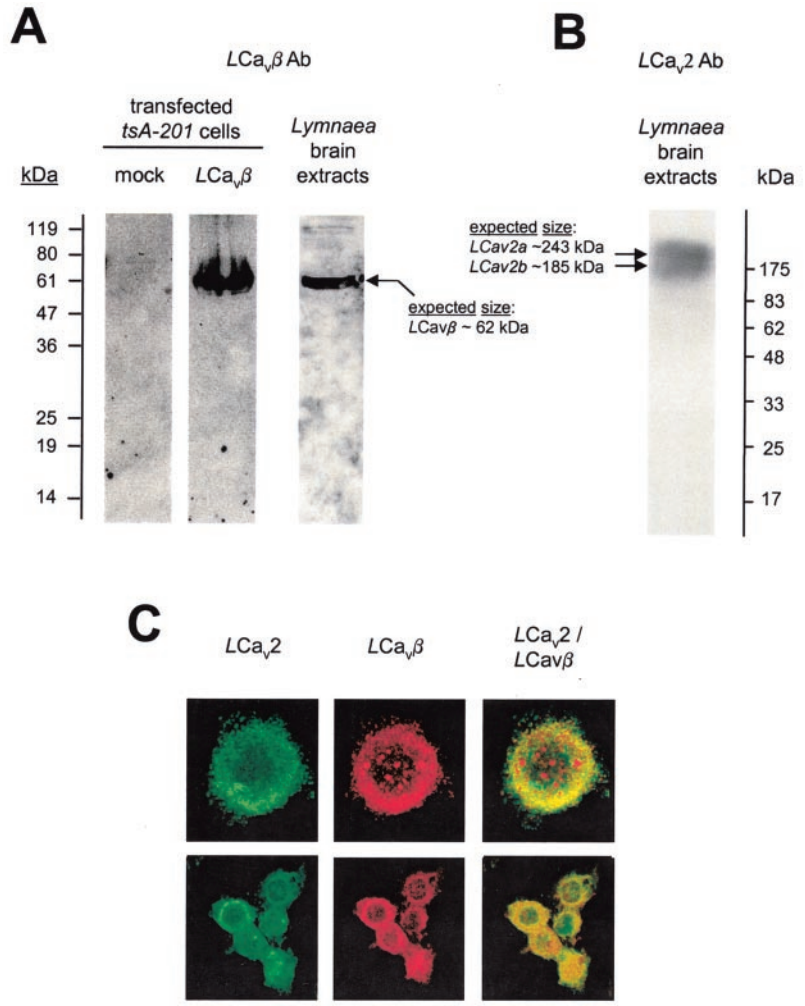


FIG. 2. **Localization of $LCa_v\beta$ and $LCa_v2$ channels with 1:2000 dilution of anti-rabbit $LCa_v\beta$ and anti-chicken $LCa_v2$ antibodies in Western blots.** *A*, identification of appropriately sized bands with $LCa_v\beta$ antibody in lanes containing protein extracts from $LCa_v\beta$-transfected *tsA-201* cells and *Lymnaea* brain *versus* a lane containing protein extracts of mock-transfected *tsA-201* cells. *B*, high molecular weight bands of expected sizes for the identified long and short $LCa_v2$ isoforms, $LCa_v2a$ and $LCa_v2b$, respectively, in lane of *Lymnaea* brain extract labeled with $LCa_v2$ antibody. *C*, overlapping (*yellow*) membrane-delimited staining of *tsA-201* cells co-transfected with $LCa_v\beta$ and $LCa_v2$ calcium channels labeled with fluorescent secondary conjugates that recognized anti-chicken $LCa_v2$ (*green*) and anti-rabbit $LCa_v\beta$ (*red*).

subunit subtypes potently regulated $LCa_v2$ function in a manner consistent with what has been reported previously for other mammalian calcium channels and β subunits (8–16). These changes include the following: 1) mild hyperpolarizing shifts in half-inactivation potential with $r\beta_{1b}$, $r\beta_3$, and $r\beta_4$ and depolarizing shifts with $r\beta_{2a}$ (Fig. 3*C*); 2) 3–6-fold increases in peak current amplitude; 3) pronounced speeding of recovery from inactivation with most rat β subunits (Fig. 3*D*); and 4) significant changes in inactivation kinetics ranging from speeding with $\beta_3$ and $\beta_{1b}$ to slowing $\beta_{2a}$ (Fig. 3*E*). Conversely, the coexpression of $LCa_v\beta$ significantly ($p < 0.05$) increased the peak current amplitudes of rat $Ca_v2$ channels ($Ca_v2.1$, from 296.7 ± 87.8 ($n = 7$) to 3060.2 ± 1359 pA ($n = 13$); $Ca_v2.2$, from 60.0 ± 12.5 ($n = 15$) to 610.5 ± 249.2 pA ($n = 13$); $Ca_v2.3$, from 136.1 ± 20.2 pA ($n = 12$) to 1123.2 ± 334.1 pA ($n = 13$)), in addition to slowing the inactivation kinetics of all rat $Ca_v2$ channels (see Fig. 3*G* for example). These data indicate that $LCa_v2$ calcium channels are susceptible to regulation by mammalian (but not invertebrate) β subunits, and more importantly, $LCa_v\beta$ subunits are indeed functional in *tsA-201* cells.

*$LCa_v2$ and $LCa_v\beta$ Distribution in Neurons*—The relative lack of effects of the expression of $LCa_v\beta$ subunits on the biophysical properties and current amplitudes of $LCa_v2$ raises the question as to whether β subunits associate with the $LCa_v2$ calcium channel in neurons. As shown in Fig. 4, antibody costaining of $LCa_v2$ channels and $LCa_v\beta$ reveals an overlapping distribution (*yellow color*) in synaptically connected identified *Lymnaea* neurons (Fig. 4*C*) with "railroad track"-like, membrane-delimited costaining of $LCa_v2$-$LCa_v\beta$ at higher magnification (Fig. 4, *E* and *F*). This indicates that in mature neurons, $LCa_v2$ calcium channels and β subunits are likely in a complex, reminiscent of what is known to occur in vertebrate neurons and consistent with the dogma that calcium channels and β subunits assemble in the ER and are cotargeted to the plasma membrane (18).

Secondary and tertiary neurites are ladened with extensive varicosities with intense $LCa_v2$-$LCa_v\beta$ colabeling, preterminally and at sites of synaptic contact (Fig. 4*D*). Most interestingly, new neurite outgrowth manifested in filopodia tufts along major neurites (Fig 4*E*, magnified in Fig. 4*F*) or emergent growth cones (Fig. 5*A*) contain mostly $LCa_v2$ staining (*green*) with a striking absence of considerable $LCa_v\beta$ staining (*red*). In terminal growth cones, a nonoverlapping distribution of $LCa_v2$ and $LCa_v\beta$ is clearly evident. In a "filopodial" type of growth cone, associated with rapidly migrating neurites (36), $LCa_v\beta$ staining emerges from the back central lamellipodium, and splays into the periphery (Fig. 5, *B* and *C*). In contrast, $LCa_v2$ is expressed in peripheral lamellipodia of growth cones (Fig. 5,

5, 6, and 13 are numbered according to the rat $\beta_3$ gene (6). Alternatively spliced long and short (a/b) isoforms exist for exons 1 and 6. The antibody epitope for $LCa_v\beta$ is indicated by *dashed box* in *A*. GenBank™ (gi) sequences for analyses includes rat isoforms: $\beta_{1b}$, 8393060; $\beta_{2a}$, 16758716; $\beta_3$, 1705686; $\beta_4$, 423788; *L. stagnalis*, 29378325; *Loligo bleekeri* 19911801; *Drosophila melanogaster* 6646874; *C. elegans* 17506267; *Schistosoma mansoni* 15283999; *Cyanea capillata* 2654496.

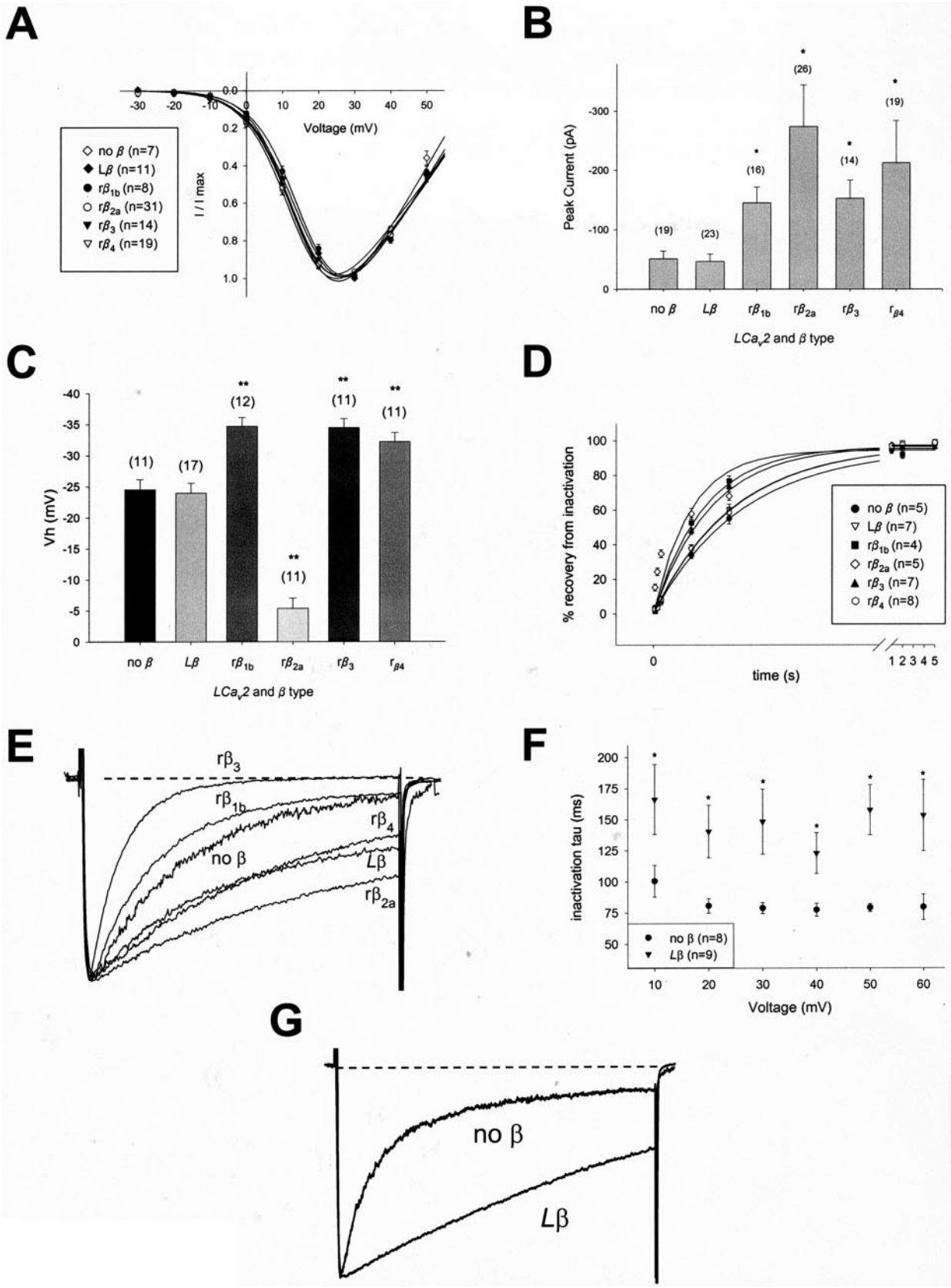


FIG. 3. *A–E*, effects of invertebrate $LCa_v\beta$ or mammalian $Ca_v\beta_1$-$\beta_4$ on biophysical characteristics of $LCa_v2$ calcium channels expressed in *tsA-201* cells. *A*, ensembles of whole cell barium current voltage relations, fitted by the Boltzmann equation. *B*, peak current amplitude of barium currents obtained at a test potential of +20 mV from a holding potential of −80 mV. *C*, half-inactivation potentials ($V_h$) obtained from Boltzmann fits to steady state inactivation curves obtained at a test potential of +20 mV. *D*, monoexponential fit of the time course of recovery from inactivation. Note that the data obtained in the presence of rat $\beta_{2a}$ are not adequately described by a monoexponential fit. *E*, representative whole cell $LCa_v2$ current traces scaled to overlap at peak to illustrate effects of various β subunits on a time course of inactivation over a 200-ms test pulse. *F*, voltage dependence of the time constant of inactivation of $LCa_v2$ barium current ($\tau$) obtained at a holding potential of −100 mV in the presence and absence of $LCa_v\beta$. *G*, representative peak current record obtained with rat $Ca_v2.3$ in the presence and the absence of $LCa_v\beta$ at a test potential of +10 mV.

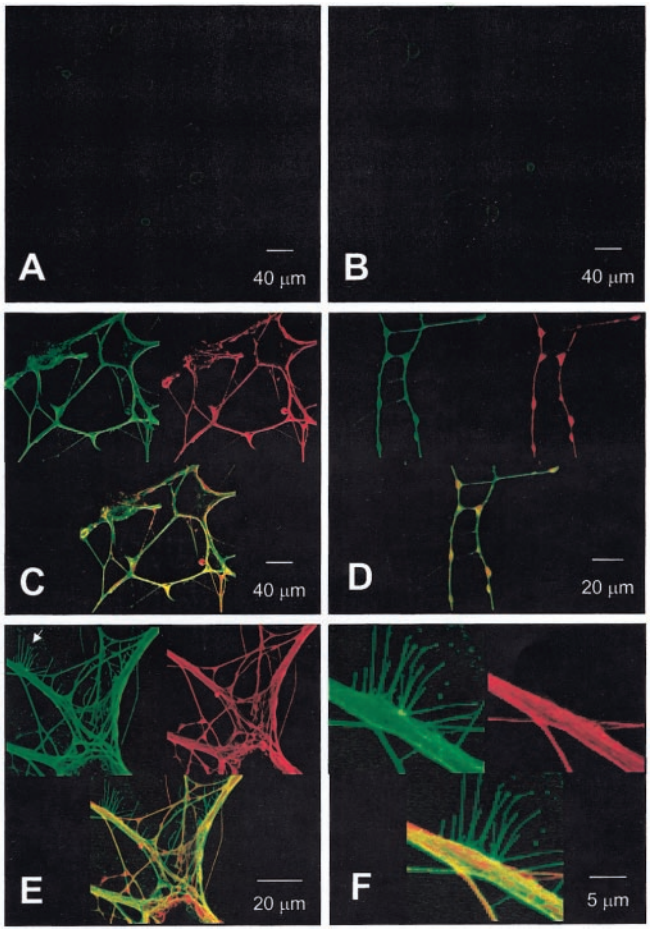


FIG. 4. **Antibody immunolocalization of the $LCa_v2$ calcium channel (anti-chicken) and $LCa_v\beta$ (anti-rabbit) in synaptically connected, identified *Lymnaea* neurons in 2-day primary cultures.** $LCa_v2$ and $LCa_v\beta$ are identified by fluorescent secondary conjugates Alexa Fluor 488 (*green, top left panel*) and 555 (*red, top right panel*), respectively (*A–F*). Superimposed antibody staining (*yellow*) displayed at bottom (*A–F*). Control staining with anti-chicken (*A*) or anti-rabbit (*B*) preimmune serum at 1:2000 dilution. Note the relative absence of staining under these control conditions. *C,* dense, double-stained $LCa_v2$ and $LCa_v\beta$ overlap (*yellow*) of synaptically paired neurons (×20); *D*, in preterminal varicosities of terminal neurites (×40). *E,* ×40 magnified sample of somata and its primary neurite offshoots; *F*, magnification of neurite with filopodia tufts (*white arrow*, in *E*).

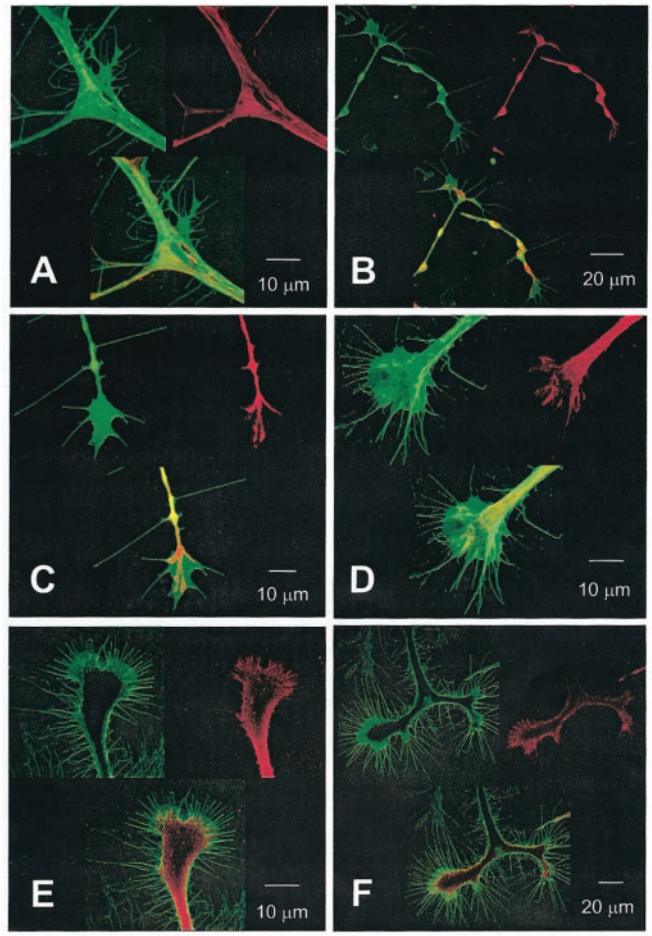


FIG. 5. **Antibody immunolocalization of $LCa_v2$ calcium channel (anti-chicken $LCa_v2$) and β subunit (anti-rabbit $LCa_v\beta$) in terminal growth cones of identified *Lymnaea* neurons in 2-day primary cultures.** $LCa_v2$ and $LCa_v\beta$ are identified by fluorescent secondary conjugates Alexa Fluor 488 (*green, top left panel*) and 555 (*red, top right panel*), respectively (*A–F*). Superimposed antibody staining (*yellow*) is displayed in the *bottom panel* (*A–F*). *A*, growth cone emerging from primary neurite (×60) and growth cones at terminal neurites (*B* = ×40; *C–F* = ×100). Dense $LCa_v2$ and $LCa_v\beta$ double-labeled staining (*yellow*) is apparent in preterminal varicosities, but nonoverlapping stain of *LCav2* (*green*) and $LCa_v\beta$ (*red*) is seen in rapidly migrating growth cones (*B–D*) where $LCa_v\beta$ is splayed from the central lamellipodium into periphery. $LCa_v2$ staining in filopodia and the peripheral lamellipodium appears as a halo surrounding $LCa_v\beta$ staining with apparent looped morphology in "paused"-type growth cones (*E* and *F*).

*B* and *C*) and filopodia emerging from both the peripheral and central region of lamellipodia (Fig. 5*D*). This distinct pattern seen with $LCa_v2$ and $LCa_v\beta$ seems reminiscent of the distinct expression patterns observed with F-actin and microtubule staining (37). In larger, "lamellipodia"-type growth cones, associated with slow migrating or paused neurites (38), a bright halo of $LCa_v2$, actin-like staining in filopodia forms around the central region of the growth cone, where $LCa_v\beta$ subunits form a microtubule-like looped pattern (Fig. 5, *E* and *F*). These data indicate that although synaptically paired neurons appear to contain complexes of $Ca_v2$ calcium channel $\alpha_1$ subunits and β subunits, the growth cone periphery and filopodia only contain the $\alpha_1$ subunit. These data thus suggest that $\alpha_1$ and β subunits may not be coassembled in the ER and transported to the membrane as stable complexes during neuronal outgrowth or, alternatively, that coassembled subunits subsequently segregate upon their arrival in growth cones.

*Role of $LCa_v2$ Channels in Growth Cones*—At synaptic nerve terminals, $LCa_v2$ channels are essential for neurotransmitter release (4) and are colocalized with β subunits. However, the function of (β subunit uncoupled) $LCa_v2$ channels in growing neurons is not known. To address this issue, we treated nonadherent cultured *Lymnaea* neurons with $LCa_v2$ RNAi or control RNAi for a period of 3 days, plated the neurons on adhesive substrate for 2 days to enable neurite outgrowth, and then post-stained for immunodetection of $LCa_v2$ and $LCa_v\beta$. Control RNAi-treated neurons ($n$ = 6) had a typical morphology with wide, rib-like, primary neurites and secondary neurites ladened with varicosities and extensions that form autapses or synapses (Fig. 6, *A* and *B*). In addition, robust colocalization of $LCa_v2$ and $LCa_v\beta$ was apparent. In the $LCa_v2$ RNAi-treated group, we observed a dramatic reduction of $LCa_v2$ antibody staining compared with control RNAi-treated neurons. All neurons adhered well to the substrate, suggesting that this subunit is not required for calcium-induced cell adhesion. However, $LCa_v2$ knockdown either eliminated all neurite growth ($n$ = 8) or produced neurons with an aberrant, stunted morphology ($n$ = 10) with either a veil-like sheath or hair-like neurites emerging from the somata (Fig. 6, *C* and *D*). In these neurons, β subunit expression was less evident in the periphery and

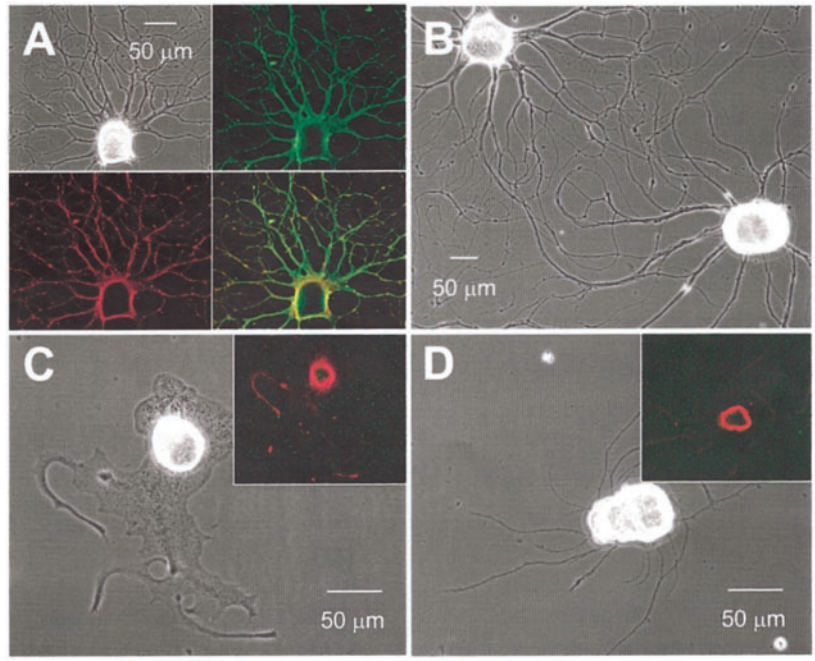


FIG. 6. **Identified cultured *Lymnaea* neurons treated with control (*A* and *B*) or $LCa_v2$ (*C* and *D*) RNAi knockdown.** *A* and *B,* control RNAi neurons show wide, rib-like, primary neurites and secondary neurites ladened with varicosities and extensions that form autapses or synapses. *A* contains bright field view, $LCa_v2$ (*green*) alone, $LCa_v\beta$ (*red*) alone, and superimposed antibody staining (*yellow*). *C* and *D, *$LCa_v2$ RNAi-treated neurons display an aberrant, stunted morphology with either a veil-like sheath (*C*) or hair-like neurites (*D*) emerging from the somata. Superimposed antibody staining of $LCa_v2$ and $LCa_v\beta$ are displayed in the *insets* (*C* and *D*).

more pronounced in the soma where L-type ($LCa_v1$) calcium channels are likely to be expressed. Overall, these data suggest that $LCa_v2$ calcium channels are required for outgrowth during neuronal differentiation. Moreover, the observation that RNAi depletion of $LCa_v2$ channels virtually abolished antibody staining further supports the specificity of the $LCa_v2$ anti-chicken antibody.

Because $LCa_v2$ channels at the tips of outgrowing neurons are not complexed with β subunits, one might expect that knockdown of $LCa_v\beta$ should not affect neuronal outgrowth. Repeated attempts with different probes for a gene knockdown using RNAi of $LCa_v\beta$ subunits did not result in a substantial reduction in $LCa_v\beta$ immunolabeling. Instead, we resorted to an antisense approach that was shown previously to lead to knockdown of mammalian β subunits (39, 40) in cultured rat dorsal root ganglion neurons. As shown in Fig. 7, *B* and *C*, antisense knockdown ($n = 8$) substantially, albeit not completely, reduced detectable $LCa_v\beta$ immunostaining compared with mismatch controls ($n = 8$). Under antisense conditions, neuronal outgrowth in treated cells was indistinguishable from control conditions (Fig. 7*A*), indicating that $LCa_v\beta$ subunit does not appear to be essential for neurite outgrowth.

*Local Synthesis of $LCa_v\beta$ in Neurites*—Our data suggest that the β subunit plays an important role upon synaptic contact, where neurites undergo cytoskeletal rearrangement to form synaptic terminals, far from the distant somata. In this context, axons may perhaps have their own mechanism for providing a rapid and ample supply of β subunits for the stabilization of calcium channel complexes upon synapse formation or synaptic remodeling during neuronal plasticity (for review see Refs. 41 and 42). To determine whether $LCa_v\beta$ could be expressed locally to associate with $LCa_v2$ and modulate its activity at synaptic terminals, we examined the localization of $LCa_v\beta$ message with radiolabeled antisense RNA. As shown in Fig. 8*A*, this analysis revealed typical somatic localization for $LCa_v\beta$ mRNA in cross-sections of the cerebral ganglion (Fig. 8*A, s*) and absence of detectable staining with a sense radiolabeled probe (not shown). Although not readily abundant, β subunit RNA could be found extrasomatically in neurites (between *white arrows,* Fig. 8*A*). To confirm the presence of $LCa_v\beta$ mRNA outside the cell body, somata were excised by glass pipette from sprouting cultured neurites of 40 identified *Lymnaea* (CGC, VD4, and LPeD1) neurons. Following the removal of somata, culture dishes containing isolated neurites were rinsed thoroughly, and RNA was extracted, PCR-amplified in a modified Eberwine protocol (43), and end-labeled to probe a membrane spotted with plasmids encoding for fragments of various $LCa_v$ channel subunits and two of the known *Lymnaea* $K_v$ channel isoforms. By using this method, a potassium channel $LK_v2.1$ (*Shab*) and $LCa_v\beta$ were detected on the blot, but surprisingly, none of the three known calcium channels (*i.e.* $LCa_v1$, $LCa_v2$, and $LCa_v3$) hybridized to neurite-derived labeled cDNA nor to $LK_v3.1$ (*KShaw*). These data indicate that the $LCa_v\beta$ subunit mRNA is present in outgrowing neurites and raises the possibility that $LCa_v\beta$ subunits might be locally translated upon synapse formation. To test this possibility, we generated a hemagglutinin (HA)-tagged $LCa_v\beta$ construct. HA-$LCa_v\beta$ mRNA was injected into soma-ablated neurites (Fig. 8, *C–E*) and monitored for expression with rat HA monoclonal antibody after a 12-h incubation. As shown in Fig. 8*F*, HA antibody staining in isolated, soma-ablated neurons was detected and overlapped with the distribution of native β subunits identified with the $LCa_v\beta$ antibody (Fig. 8, *G* and *H*). The greatest density of β subunit staining was found at the site of mRNA injection (Fig. 8, *E* and *F*). In contrast, soma-ablated neurites that were not injected with HA-$LCa_v\beta$ mRNA were not subject to detectable HA antibody staining (data not shown). These data support the idea that $LCa_v\beta$ subunits can be locally synthesized for possible complex formation with calcium channels in nascent synapses or after synaptic remodeling.

## DISCUSSION

We present several novel findings concerning $LCa_v2$ channels and their association with β subunits. First, the singleton representative of β subunits in *Lymnaea* neurons was not capable of strongly modulating the biophysical characteristics nor the whole cell current amplitude of $LCa_v2$ channels in *tsA-201* cells, suggesting that the fundamental role of this subunit may be unrelated to altering channel function *per se*. Whether this absence of strong modulation is also a characteristic of the other high voltage-gated channel in *Lymnaea*, $LCa_v1$ is not addressed here. Second, although $LCa_v2$ and $LCa_v\beta$ colocalize in mature, synaptically connected neurons, the $LCa_v2$ $\alpha_1$ subunit is decoupled from the β subunit in ter-

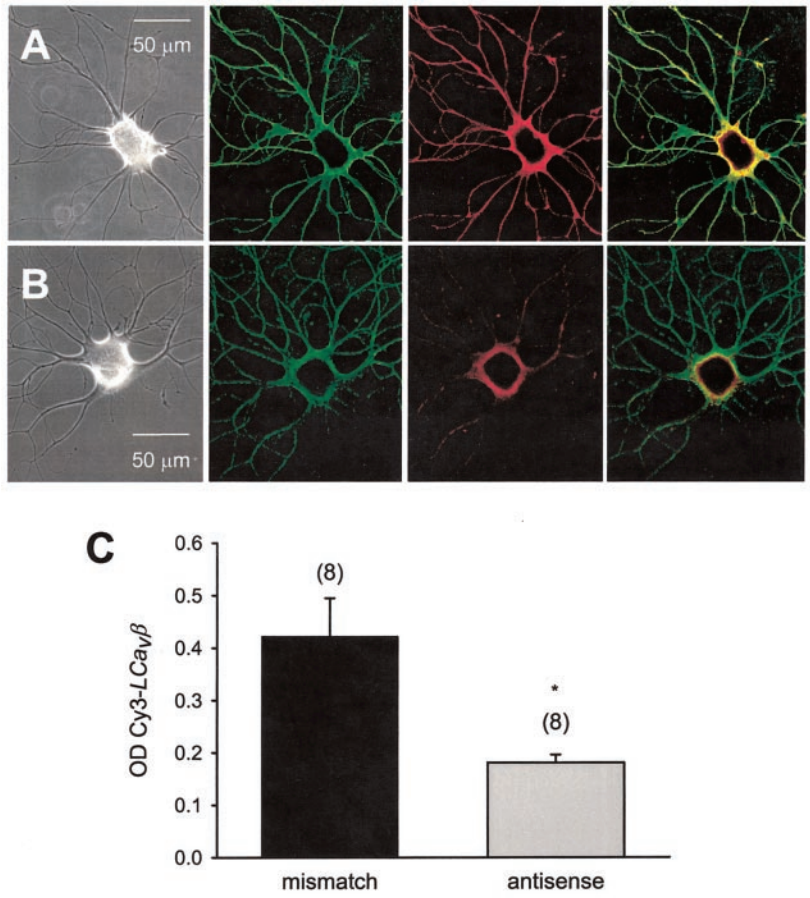


FIG. 7. Identified *Lymnaea* culture neurons treated with mismatch (*A*) or antisense (*B*) $LCa^{v}\beta$. Each panel contains a bright field view and immunodetection of $LCa_v2$ (*green*), $LCa_v\beta$ (*red*), and superimposed antibody staining (*yellow*). Representative sample illustrates substantial reduction of detectable *LCavβ* immunostaining with antisense (*B*) compared with mismatch controls (*A*) with no measurable effect on neurite outgrowth. *C*, fluorescence intensities of antisense *versus* mismatch $LCa_v\beta$ antibody staining were quantified in optical density units in a 200 × 200 μm area encompassing each neuron centered in view.

minal growth cones and nascent growth along major neurites. Third, the message for the β subunit was detected outside the cell soma and can be locally translated in neurites. Finally, the expression of a calcium channel subtype that is normally associated with neurotransmitter release is essential for appropriate neuronal outgrowth.

It is well established that presynaptic (*i.e.* $Ca_v2$) voltage-gated calcium channels can tightly associate with ancillary β subunits. Localization with specific antibodies and mRNA analyses revealed that neurons express all of the known β subunit genes (*i.e.* $\beta_1$ to $\beta_4$) (23–25), and each of these different β subunit isoforms can, at least in transient expression systems, functionally associate with both N-type ($Ca_v2.2$) and P/Q-type ($Ca_v2.1$) calcium channels (8, 12, 14), the major calcium channels involved in the release of neurotransmitters from presynaptic nerve termini (1). In expression systems, β subunit coexpression has been shown to affect not only the biophysical properties of various calcium channel $\alpha_1$ subunits (such as activation and inactivation) but, perhaps more importantly, to promote increased current densities (for reviews see Refs. 6 and 7), suggesting a role of β subunits in membrane trafficking of the $\alpha_1$ subunit (18). The functional significance of β subunits in neurons is further supported by analyses of knockout and mutant mice (5). Knockout of $\beta_3$ reduces the activities of neuronal L-type and N-type channels (20). The *lethargic* mouse, an effective $\beta_4$ null mutant, is characterized by seizure activity and ataxia; however, the density of presynaptic calcium channels is not affected possibly because of compensation from other β subunit subtypes (19, 44). Indeed, the combinatorial complexity of multiple β and $\alpha_1$ subunits has prevented detailed insights into the precise function of β subunits in synaptic terminals *in vivo* (21).

Unlike the four vertebrate β subunit genes, only singleton homologs have been identified in sequenced invertebrate genomes (*Drosophila* and *C. elegans*) and six other invertebrates from five diverse phyla (see Fig. 1*B*). β subunits have been linked with other gene families to a HOX gene cluster, whose different subtypes, like $\beta_1$ through $\beta_4$ are spread between four tightly packed paralogous segments, which likely arose through two rounds of duplication from a linked cluster of a single, ancestral invertebrate-type gene (45). These data are thus consistent with the presence of the β subunit singleton identified in the *Lymnaea* brain. Furthermore, in repeated attempts, we failed to isolate a second *Lymnaea* β subunit isoform using degenerate PCR of freshly isolated cDNA or hybridization screening of cDNA libraries. As with the β subunit, invertebrates (*i.e. C. elegans*, *Drosophila*, and *Lymnaea*) express only a single $Ca_v2$ homolog, which represents structurally and functionally the vertebrate $Ca_v2.1$, $Ca_v2.2$, and $Ca_v2.3$ calcium channels (2–4). Because of the reduced complexity, invertebrates such as *Lymnaea* therefore have the capacity to provide unique insights into the roles of calcium channel $\alpha_1$ and β subunits in synaptic physiology.

We have recently shown that $LCa_v2$ calcium channels are essential for synaptic transmission at cholinergic synapses between identified *Lymnaea* neurons and, specifically, that this involved a splice isoform of $LCa_v2$ that is capable of interacting with the scaffolding proteins Mint-1 and CASK (4). Together with work in rat hippocampal neurons (46), this suggested that membrane-associated guanylate kinase scaffolding proteins with PDZ, SH3, and guanylate kinase domains such as CASK are likely involved in targeting and stabilizing $Ca_v2$ calcium channels to synaptic contacts. It is interesting to note that calcium channel β subunits also contain membrane-associated guanylate kinase-like SH3 and guanylate kinase domains (33–35), raising the possibility that secondary interactions of β

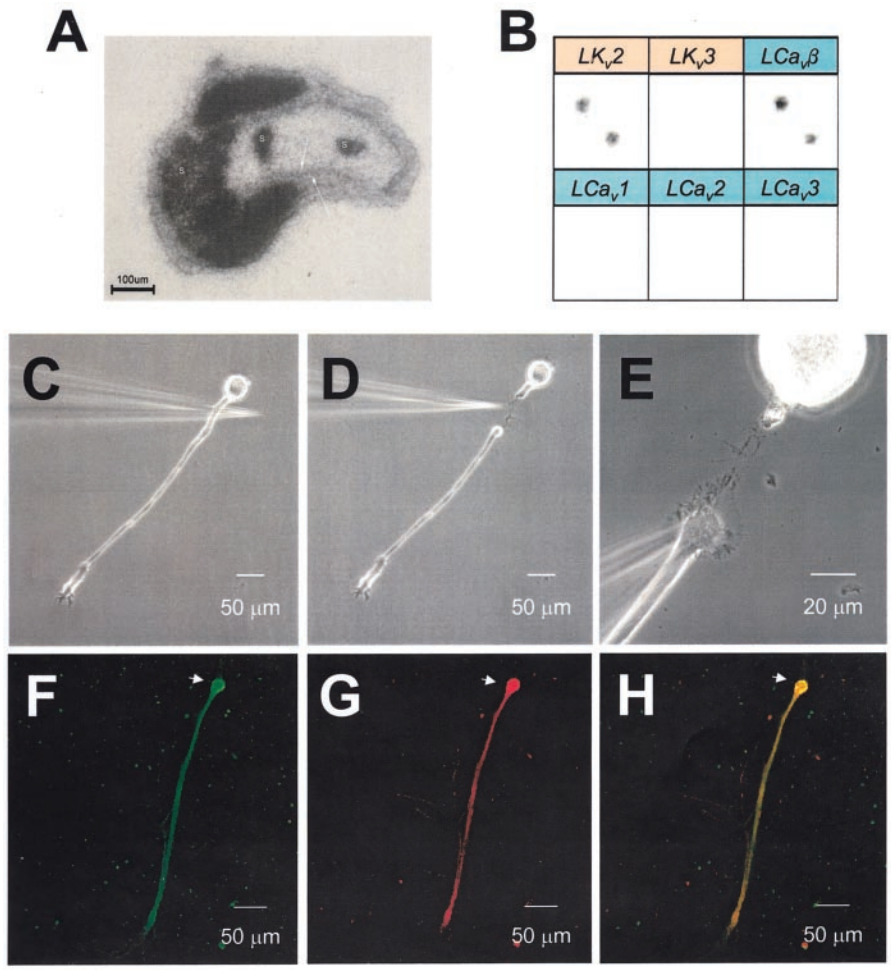


FIG. 8. **Identification of β subunit mRNAs and local translation capacity in *Lymnaea* neurites.** *A*, localization of $^{35}$S-dUTP-labeled antisense $LCa_v\beta$ RNA in a diagonal tissue section through cerebral ganglia and connecting commissure. Note abundant staining in cell soma (s) but detectable quantity also in neurites (between *white arrows*). *B*, reverse Northern blot containing spotted cDNA fragments of *Lymnaea* $K_v2.1$ (*KShab*), $K_v3.1$ (*KShaw*), and $LCa_v1$–*3* and $LCa_v\beta$, probed with PCR-amplified $^{32}$P-labeled cRNA from soma-ablated neurites (see illustration in *C* and *D*). Note the selective hybridization of $LK_v3$ and $LCa_v\beta$ with neuritic probe. *C* and *D*, illustration of soma ablation with sterile glass pipette of identified CGC neurons after 2 days in culture. *E*, injection of the neurite shown in *C* with mRNA of hemagglutinin-tagged $LCa_v\beta$ followed by fixation and immunohistochemistry of neurite (*F*–*H*) after 12 h. Fluorescent secondary conjugates were chosen to recognize a rat HA monoclonal antibody (*F*). Note that the staining density is highest at the site of mRNA injection. *G*, staining of neurite with anti-rabbit *LCavβ*. *H*, superposition of *F* and *G*.

subunits with scaffolding proteins may aid in stabilizing and anchoring of $LCa_v2$ calcium channels in synaptic terminals.

In contrast, nascent growth along major neurites contained $LCa_v2$ channels in filopodia without associated β subunits. Indeed, there was a clear separation of $\alpha_1$ and β subunits in terminal growth cones, and knockdown of the β subunit did not affect neuronal growth *per se*, suggesting that β subunits do not play the same role as $LCa_v2$ channels during neurite outgrowth. The expression pattern of $\alpha_1$ and β subunits, respectively, bore a striking resemblance to those described previously for actin and tubulin (37, 47). It is thus tempting to speculate that targeting of $\alpha_1$ and β subunits to their appropriate positions in growth cones could be mediated through interactions with these cytoskeletal elements. Actin and microtubule dynamics are associated with cellular processes that involve structural rearrangements, such as cell motility and division, and they enable rapid intracellular reorganization in shape and direction in growth cones in response to external cues (47). A close association of β subunits and $LCa_v2$ channels with these motile proteins would result in their redistribution along with the dynamic shape and direction changes in growth cones. Although we do not have any experimental evidence that calcium channel subunits are directly associated with actin and tubulin, there are at least some indications from the literature in support of such a mechanism. For example, CASK, which physically binds to $Ca_v2$ calcium channels, is indirectly coupled to actin/spectrin microfilaments (48). Moreover, Gem, a small GTP-binding protein, localizes with actin and microtubules (49) and can associate with mammalian calcium channel β subunits, rendering them inoperative. As a consequence, activated Gem will inhibit mammalian calcium channels (50). It is possible that similar cytoskeletal linked regulatory proteins may modulate the interactions between $Ca_v2$ channels and β subunits.

The observation that knockdown of the $LCa_v2$ $\alpha_1$ subunit resulted in drastically impaired neuronal growth is consistent with observations from a *Drosophila* $Ca_v2$ mutant ($Dmca1A^{NT27}$) that produces a 35% reduction in terminal branching in neuromuscular junction synapses, and a reduced number in varicosities (51). Similarly, in $Ca_v2.1$ mouse mutants such as the Rocker mouse, Purkinje neurons show a dramatic reduction of dendritic arborization (52). In contrast, the $\beta_4$ *lethargic* null mutant mouse, which bears the same ataxia and seizure phenotype as the Rocker mouse (probably because of impaired transmitter release in both types of mice), has no apparent structural neuropathology (19, 44). The phenotypes of these mutants are thus consistent with the idea that $Ca_v2$, but not the β subunit, mediates a role in neuronal growth. It seems likely that the role of $Ca_v2$ channels in neurite outgrowth is linked to a reduction in calcium influx in growth cones. Indeed, mammalian voltage-gated calcium channels are known to play a role in spontaneous depolarization "transients" that mediate axonal branching (53) and growth cone extension and guidance to external cues (54). Although these transients are reportedly dihydropyridine-sensitive (thus suggesting an involvement of L-type channels), it is not yet clear to what extent $Ca_v2$ channels may be involved in this phenomenon.

At this point, the significance of the absence of β subunits in the periphery of growth cones and filopodia is unknown. It is plausible, however, that the dynamic nature of the growth cone requires a complement of highly motile calcium channel $\alpha_1$ subunits, in contrast with mature synaptic contacts where

calcium channels must be precisely and permanently localized to the active zone. This would fit with the idea of the calcium channel β subunit as a regulator of $\alpha_1$ subunit stability/mobility. Local protein synthesis in axons and dendrites provides independence from the distant soma to support a rapid supply of proteins for changing conditions in neurites, such as axonal branching, growth cone guidance, and synapse formation (41, 42). Within this framework, the observation that the β subunit can potentially be synthesized locally may provide a mechanism by which this subunit could assemble with existing $LCa_v2$ channels following the establishment of synaptic contacts, thus maintaining the precise localization of the $\alpha_1$ subunit in the nerve terminal. It is also known that the induction of long term potentiation activates the local translation of mRNA encoding for factors that mediate synaptic plasticity (42). It is thus tempting to speculate that the local synthesis of β subunits also may be critical during depolarization-induced remodeling of synapses.

It has been suggested that the β subunit masks an ER retention signal on the $\alpha_1$ subunit that prevents efficient plasma membrane targeting of the $\alpha_1$ subunit (18). If so, then the observation that $LCa_v2$ $\alpha_1$ subunits are uncoupled from β subunits in growth cones would imply that β subunits dissociate from $\alpha_1$ subunits in growth cones. Alternatively, it is possible that membrane trafficking of $\alpha_1$ subunits can occur altogether independently of β subunits. Indeed, although it is true that surface expression of certain $\alpha_1$ subunits in transient expression systems is increased with β subunits (18, 55), and that β subunit knockout mice often have reduced calcium current densities (5), there is no direct evidence for ER retention in neurons. The differential localization of $\alpha_1$ and β subunits in growth cones, together with the findings that membrane expression did not appear to be altered in *tsA-201* cells following $LCa_v\beta$ coexpression (*i.e.* current densities were unaffected) and that robust membrane expression of $LCa_v2$ was observed in β subunit antisense-depleted neurons, is also inconsistent with $LCa_v\beta$ being required for efficient translocation of calcium channels from the ER.

Divergence of β subunit sequences has permitted multiple modulatory functions of β subunits, which act in a cell type and calcium channel-specific manner (6, 7). However, the virtual structural invariance of the β subunit core across divergent species and its resemblance to a membrane-associated guanylate kinase scaffolding molecule suggests that a primary role of the β subunit may be to stabilize membrane protein complexes associated with high voltage-activated calcium channels. Our data show that in the central nervous system, $Ca_v2$ calcium channels have both a role in mature synapses to mediate neurotransmitter release (4) and an apparent role to regulate growth of developing neurons. The differential association of β subunits with synaptic calcium channels and those expressed in emergent neuronal growth suggests that the β subunit may mediate the transformation of $Ca_v2$ calcium channel function in immature neurons and mature synapses.

*Acknowledgments*—We thank Ronald van Kesteren (Vrije Universiteit Amsterdam, The Netherlands) and Sarah McFarlane (University of Calgary) for helpful input for this paper.

REFERENCES


1. Luebke, J. I., Dunlap, K., and Turner, T. J. (1993) *Neuron* **11,** 895–902
2. Kawasaki, F., Felling, R., and Ordway, R. W. (2000) *J. Neurosci.* **20,** 4885–4889
3. Schafer, W. R., and Kenyon, C. J. (1995) *Nature* **375,** 73–78
4. Spafford, J. D., Munno, D. W., Van Nierop, P., Feng, Z. P., Jarvis, S. E., Gallin, W. J., Smit, A. B., Zamponi, G. W., and Syed, N. I. (2003) *J. Biol. Chem.* **278,** 4258–4267
5. Arikkath, J., and Campbell, K. P. (2003) *Curr. Opin. Neurobiol.* **13,** 298–307
6. Birnbaumer, L., Qin, N., Olcese, R., Tareilus, E., Platano, D., Costantin, J., and Stefani, E. (1998) *J. Bioenerg. Biomembr.* **30,** 357–375
7. Dolphin, A. C. (2003) *J. Bioenerg. Biomembr.* **35,** 599–620
8. Berrow, N. S., Brice, N. L., Tedder, I., Page, K. M., and Dolphin, A. C. (1997) *Eur. J. Neurosci.* **9,** 739–748
9. Castellano, A., Wei, X., Birnbaumer, L., and Perez-Reyes, E. (1993) *J. Biol. Chem.* **268,** 12359–12366
10. Chien, A. J., Zhao, X., Shirokov, R. E., Puri, T. S., Chang, C. F., Sun, D., Rios, E., and Hosey, M. M. (1995) *J. Biol. Chem.* **270,** 30036–30044
11. De Waard, M., Pragnell, M., and Campbell, K. P. (1994) *Neuron* **13,** 495–503
12. De Waard, M., and Campbell, K. P. (1995) *J. Physiol.* (*Lond.*) **485,** 619–634
13. Neely, A., Wei, X., Olcese, R., Birnbaumer, L., and Stefani, E. (1993) *Science* **262,** 575–578
14. Stea, A., Dubel, S. J., Pragnell, M., Leonard, J. P., Campbell, K. P., and Snutch, T. P. (1993) *Neuropharmacology* **32,** 1103–1116
15. Stotz, S. C., Barr, W., McRory, J. E., Chen, L., Jarvis, S. E., and Zamponi, G. W. (2004) *J. Biol. Chem.* **279,** 3793–3800
16. Takahashi, S. X., Mittman, S., and Colecraft, H. M. (2003) *Biophys. J.* **84,** 3007–3021
17. Yasuda, T., Chen, L., Barr, W., McRory, J. E., Lewis, R. J., Adams., D. J., and Zamponi, G. W. (2004) *Eur. J. Neurosci.* **20,** 1–13
18. Bichet, D., Cornet, V., Geib, S., Carlier, E., Volsen, S., Hoshi, T., Mori, Y., and De Waard, M. (2000) *Neuron* **25,** 177–190
19. Burgess, D. L., Biddlecome, G. H., McDonough, S. I., Diaz, M. E., Zilinski, C. A., Bean, B. P., Campbell, K. P., and Noebels, J. L. (1999) *Mol. Cell. Neurosci.* **13,** 293–311
20. Namkung, Y., Smith, S. M., Lee, S. B., Skrypnyk, N. V., Kim, H. L., Chin, H., Scheller, R. H., Tsien, R. W., and Shin, H. S. (1998) *Proc. Natl. Acad. Sci. U. S. A.* **95,** 12010–12015
21. Miller, R. J. (2001) *Trends Neurosci.* **24,** 445–449
22. Timmermann, D. B., Westenbroek, R. E., Schousboe, A., and Catterall, W. A. (2002) *J. Neurosci. Res.* **67,** 48–61
23. Ludwig, A., Flockerzi, V., and Hofmann, F. (1997) *J. Neurosci.* **17,** 1339–1349
24. Scott, V. E., De Waard, M., Liu, H., Gurnett, C. A., Venzke, D. P., Lennon, V. A., and Campbell, K. P. (1996) *J. Biol. Chem.* **271,** 3207–3212
25. Witcher, D. R., De Waard, M., Liu, H., Pragnell, M., and Campbell, K. P. (1995) *J. Biol. Chem.* **270,** 18088–18093
26. Spafford, J. D., and Zamponi, G. W. (2003) *Curr. Opin. Neurobiol.* **13,** 308–314
27. Spafford, J. D., Chen, L., Feng, Z. P., Smit, A. B., and Zamponi, G. W. (2003) *J. Biol. Chem.* **278,** 21178–21187
28. Feng, Z. P., Klumperman, J., Lukowiak, K., and Syed, N. I. (1997) *J. Neurosci.* **17,** 7839–7849
29. Smit, A. B., Syed, N. I., Schaap, D., van Minnen, J., Klumperman, J., Kits, K. S., Lodder, H., van der Schors, R. C., van Elk, R., Sorgedrager, B., Brejc, K., Sixma, T. K., and Geraerts, W. P. (2001) *Nature* **411,** 261–268
30. Syed, N. I., Ridgway, R. L., Lukowiak, K., and Bulloch, A. G. (1992) *Neuron* **8,** 767–774
31. Spencer, G. E., Syed, N. I., van Kesteren, E., Lukowiak, K., Geraerts, W. P., and van Minnen, J. (2000) *J. Neurobiol.* **44,** 72–81
32. van Kesteren, R. E., Syed, N. I., Munno, D. W., Bouwman, J., Feng, Z. P., Geraerts, W. P., and Smit, A. B. (2001) *J. Neurosci.* **21,** RC161
33. Chen, Y. H., Li, M. H., Zhang, Y., He, L. L., Yamada, Y., Fitzmaurice, A., Shen, Y., Zhang, H., Tong, L., and Yang, J. (2004) *Nature* **429,** 675–680
34. Hanlon, M. R., Berrow, N. S., Dolphin, A. C., and Wallace, B. A. (1999) *FEBS Lett.* **445,** 366–370
35. Van Petegem, F., Clark, K. A., Chatelain, F. C., and Minor, D. L. (2004) *Nature* **429,** 671–675
36. Letourneau, P. C. (1983) *J. Cell Biol.* **97,** 963–973
37. Bridgman, P. C., and Dailey, M. E. (1989) *J. Cell Biol.* **108,** 95–109
38. Tsui, H. T., Lankford, K. L., Ris, H., and Klein, W. L. (1984) *J. Neurosci.* **4,** 3002–3013
39. Berrow, N. S., Campbell, V., Fitzgerald, E. M., Brickley, K., and Dolphin, A. C. (1995) *J. Physiol* (*Lond.*) **482,** 481–491
40. Campbell, V., Berrow, N. S., Fitzgerald, E. M., Brickley, K., and Dolphin, A. C. (1995) *J. Physiol.* (*Lond.*) **485,** 365–372
41. Giuditta, A., Kaplan, B. B., van Minnen, J., Alvarez, J., and Koenig, E. (2002) *Trends Neurosci.* **25,** 400–404
42. Richter, J. D., and Lorenz, L. J. (2002) *Curr. Opin. Neurobiol.* **12,** 300–304
43. Diatchenko, L., Chenchik, A., and Siebert, P. D. (1996) in *Gene Cloning and Analysis* (Siebert, P. D., and Larrick, J., eds) pp. 213–239, Biotechniques Books, Natick, MA
44. Burgess, D. L., Jones, J. M., Meisler, M. H., and Noebels, J. L. (1997) *Cell* **88,** 385–392
45. Escayg, A., Jones, J. M., Kearney, J. A., Hitchcock, P. F., and Meisler, M. H. (1998) *Genomics* **50,** 14–22
46. Maximov, A., and Bezprozvanny, I. (2002) *J. Neurosci.* **22,** 6939–6952
47. Dent, E. W., and Gertler, F. B. (2003) *Neuron* **40,** 209–227
48. Biederer, T., and Sudhof, T. C. (2001) *J. Biol. Chem.* **276,** 47869–47876
49. Piddini, E., Schmid, J. A., de Martin, R., and Dotti, C. G. (2001) *EMBO J.* **20,** 4076–4087
50. Beguin, P., Nagashima, K., Gonoi, T., Shibasaki, T., Takahashi, K., Kashima, Y., Ozaki, N., Geering, K., Iwanaga, T., and Seino, S. (2001) *Nature* **411,** 701–706
51. Rieckhof, G. E., Yoshihara, M., Guan, Z., and Littleton, J. T. (2003) *J. Biol. Chem.* **278,** 41099–41108
52. Zwingman, T. A., Neumann, P. E., Noebels, J. L., and Herrup, K. (2001) *J. Neurosci.* **21,** 1169–1178
53. Tang, F., Dent, E. W., and Kalil, K. (2003) *J. Neurosci.* **23,** 927–936
54. Hong, K., Nishiyama, M., Henley, J., Tessier-Lavigne, M., and Poo, M. (2000) *Nature* **403,** 93–98
55. Altier, C., Dubel, S. J., Barrere, C., Jarvis, S. E., Stotz, S. C., Spaetgens, R. L., Scott, J. D., Cornet, V., De Waard, M., Zamponi, G. W., Nargeot, J., and Bourinet, E. (2002) *J. Biol. Chem.* **277,** 33598–33603